Investigation of the initial deposition steps and the interfacial layer of Atomic Layer Deposited (ALD) Al 2 O 3 on Si

Georgios Gakis, Constantin Vahlas, Hugues Vergnes, Sandrine Dourdain, Yann Tison, Hervé Martinez, Jerôme Bour, David Ruch, Andreas Boudouvis, Brigitte Caussat, et al.

Applied Surface Science 492 (2019) 245–254

Full length article

Investigation of the initial deposition steps and the interfacial layer of Atomic Layer Deposited (ALD) Al_2O_3 on Si

Georgios P. Gakis[a,b], Constantin Vahlas[c], Hugues Vergnes[b], Sandrine Dourdain[d], Yann Tison[e], Hervé Martinez[e], Jérôme Bour[f], David Ruch[f], Andreas G. Boudouvis[a], Brigitte Caussat[b,*], Emmanuel Scheid[g]

[a] National Technical University of Athens, School of Chemical Engineering, Heroon Polytechneiou 9, 15780, Zografou, Athens, Greece
[b] Laboratoire de Génie Chimique, Université de Toulouse, 4 allée Emile Monso, 31030 Toulouse cedex 4, France
[c] CIRIMAT, Université de Toulouse, 4 allée Emile Monso, 31030 Toulouse cedex 4, France
[d] ICSM, CEA, CNRS, ENSCM, Université de Montpellier, 30207 Bagnols-sur-Cèze, France
[e] IPREM ECP-UMR CNRS, Université de Pau et des Pays de l'Adour, Hélioparc Pau-Pyrénées, 2 Avenue du Président Angot, 64053 Pau Cedex 9, France
[f] Luxembourg Institute of Science and Technology (LIST), ZAE Robert Steichen, 5 rue Bommel, L-4940 Hautcharage, Luxembourg
[g] LAAS, Université de Toulouse, 7 avenue du Colonel Roche, 31031 Toulouse, France

ARTICLE INFO

Keywords:
ALD
TMA
Alumina
Silicon
Interface
Island growth

ABSTRACT

During the first stages of Atomic Layer Deposition (ALD) of Al_2O_3 on silicon (Si), the substrate nature affects the surface chemistry, leading to an initial island growth mode. Furthermore, an interfacial zone develops between the Si surface and the dielectric, thus damaging the physical properties of the deposited structure. In this work, these two main shortcomings are investigated for the ALD of Al_2O_3 films on Si from TMA and H_2O. The film and the interfacial zone are characterized by a complete range of techniques, including XRR, TEM, XPS, EDX and ToF-SIMS. In parallel, a computational model is developed to study the initial nucleation and growth steps of the film. An induction period is experimentally evidenced and numerically reproduced, together with the island growth and coalescence phenomena. The chemical composition of the (Al, O, Si) interfacial layer is precisely analyzed to get insight in the mechanisms of its formation. We show that Si oxidation occurs during the island growth, catalyzed by the presence of Al, while it is also fed by species interdiffusion through the ALD film.

1. Introduction

During the last two decades, the constant shrinking of electronic devices requires the production of conformal ultra-thin film structures, able to answer to the demands of the microelectronic industry [1]. The high k gate oxides used for the transistor gate stack in microelectronic devices need to be highly uniform and pinhole-free on the semi-conductor surface (Si) to prevent leakage current [1]. Within this context, the Atomic Layer Deposition (ALD) process [2] has emerged as the appropriate process to produce such films.

ALD is a film deposition technique based on the sequential use of self-terminating gas–solid reactions [3]. The advantage of ALD relies on the self-saturating chemisorption of the reactants on the surface, which ensures a high control over the thickness of the deposited film [2]. A wide variety of materials has been deposited by ALD [3], making it a powerful tool in thin film deposition technologies.

One of the most studied ALD processes is the deposition of Al_2O_3 films, using tri-methyl aluminum ($Al(CH_3)_3$, TMA) and H_2O vapor as a metal precursor and oxidant source, respectively [3]. Al_2O_3 is a favor-able candidate to replace SiO_2 as a dielectric layer as it has a higher dielectric constant and has a similar band gap [4]. A great number of works has been published on this ALD process, dealing with the de-position process [5–7], reaction mechanisms [8–10], reaction kinetics [11–13], as well as the ALD reactor dynamics [13–15].

However, even for these well-known ALD Al_2O_3 films, the deposi-tion is non ideal. Specifically, during the first stages of Al_2O_3 ALD from TMA and H_2O, an induction period has been reported on HF-cleaned Si [16,17]. This has been attributed to an island growth of the film during the initial cycles [17] which has also been reported for other materials [18]. In this regime, a minimum number of cycles is needed to obtain a conformal and continuous film, making difficult the deposition of ultra-thin, i.e. thinner than 3 nm, films on clean silicon. This regime has been studied both experimentally [16,18,19], and theoretically, with the use of computational models [16,17,20]. The analysis of the nucleation and

* Corresponding author.
E-mail address: brigitte.caussat@ensiacet.fr (B. Caussat).

growth steps during the first ALD cycles, however, remains crucial for the understanding of the inhibition mechanisms and thus the deposition of conformal, nanometric thin films.

In addition to the induction period and the non-layer by layer growth, during the first steps of the ALD process, an interfacial layer is formed between the deposited alumina film and the Si substrate. This interface is of great importance, as it can affect the electrical properties of the dielectric film [21], and thus its applications. Even though this interfacial layer is thicker for films grown with O_3 or O_2 plasma [21,22], it is nonetheless formed when using H_2O as the oxygen source [4,21–24]. The mechanisms involved are not well understood. Nau-mann et al. [24] reported an interfacial layer containing SiO_x and OH, formed during the initial deposition steps. According to their work, the OH groups formed during the initial stages of deposition enhance substrate oxidation. After the ALD layer formation, O diffusion through alumina leads to further interfacial oxide growth. Renault et al. [4] reported a thin interface, consisting mainly of SiO_x in multiple oxida-tion states. They assigned interfacial oxidation to Al-OH groups that serve as bulk defects and enhance Si oxidation and O diffusion. Inter-facial oxide regrowth during thermal annealing has also been reported [4,24,25]. Gosset et al. [25] showed the presence of Al, C, OH and H in the interface, thus showing the complex chemical composition of this layer. This interface has a negative impact, as it affects the electrical properties of the deposited structure, exhibiting a low dielectric con-stant and high leakage current for thin films below 4 nm [21], thus limiting the interest for potential applications of such films.

In this work, we deposit Al_2O_3 films via ALD, using TMA and H_2O as reactants, in a commercial ALD reactor. The films, obtained after var-ious numbers of cycles, are characterized by X-ray Reflectivity (XRR), Transmission Electron Microscopy (TEM) and Scanning Transmission Electron Microscopy in Bright Field mode (BF-STEM). As a substrate inhibited growth is observed during the first ALD cycles, we develop a computational model, inspired by the work of Nilsen et al. [20], si-mulating the island growth on the surface. The island growth for the ALD of alumina has been studied theoretically before [16,17], but with phenomenological models. The present model is based only on geo-metric principles, as that of Nilsen et al. [20] and takes into account the three dimensional aspects of the growth. Information about the growth regime, island coalescence, and surface concentration of nucleation sites are extracted from this analysis.

Information about the interfacial layer formation as a function of the number of cycles and film deposition is also drawn from the ex-perimental analysis, illuminating certain aspects of its formation me-chanisms. The depth profile of the deposited film and its interface in terms of elemental composition is studied using Energy Dispersive X-ray spectroscopy (EDX), X-ray Photoelectron Spectroscopy (XPS) and Time of Flight Secondary Ion Mass Spectrometry (ToF-SIMS) char-acterizations, yielding information on its chemical nature. The results about the interfacial layer formation and its composition can serve as valuable information for restricting its formation by applying adequate surface pre-treatments for Si.

2. Materials and methods

The Al_2O_3 films were deposited using a commercial Veeco® Fiji F200 ALD setup, on 100 mm diameter Si (100) wafers. The wafers were pretreated by deionized (DI) water rinsing, followed by dipping in a 5% HF solution for 1 min, in order to remove the native oxide on the Si surface, and a final DI water rinsing. After the pretreatment, the wafer was dried and immediately loaded into the chamber, which was pumped out to its base pressure (10^{-4}–10^{-5} Torr) for 10 min, then to the base pressure of the ALD process (0.072 Torr) with Ar nominal flows for 5 min.

The TMA pulse time was set to 0.025 s, while the water pulse was 0.1 s. The two reactant exposures were separated by an Ar purging step of 5 s. The pulsing and purging times being set, the isolation valve of the capacitance manometer was closed. The number of cycles used varied from 5 to 550. The substrate temperature was kept at 300 °C, for all samples. This process recipe has been studied before [13] and yields a steady state growth per cycle of ~0.1 nm/cycle. For more information about the deposition mechanisms and the process setup, the reader is referred to our previous works [13,14].

The thickness of the deposited films was measured by two means. Firstly, for some samples we used Transmission Electron Microscopy (TEM) and Bright Field Scanning TEM (BF-STEM) with a 200 kV JEOL JEM-ARM200F Cold FEG microscope, coupled to an Energy-dispersive X-ray spectroscope (EDX), which was used for the chemical character-ization of the films. The cross section preparation was done by Focused Ion Beam (FIB) milling in a FEI Helios Nanolab 600i dual beam SEM/ FIB. For the TEM and STEM analysis, the Al_2O_3 film was capped by a 30 nm carbon layer using an electron beam, followed by a 3 μm Pt layer deposited with an ion beam.

Secondly, we systematically used X-ray reflectivity measurements, which were carried out using a Bruker D8 diffractometer with Cu Kα1 (λ = 0.154056 nm) radiation. All measurements were carried out in $\theta - \theta$ geometry for which the sample was kept fixed during the mea-surements. Experimental curves were fitted using reflex software [37] based on the Parratt algorithm to obtain the thickness and the electron density profile of the prepared layer.

In order to analyze the film composition as a function of the film depth, dynamic SIMS analysis was performed using a ToF SIMS V (IonToF, Münster, Germany). For the depth profile measurement, a 25 keV pulsed Bi3+ cluster ion source delivering 0.31 pA of target current was used for the analysis while a 3 keV Cs + source was oper-ated for the sputtering with 20 nA target current. The sputtered crater size was 250 μm × 250 μm and only a 100 μm × 100 μm area in the middle was analyzed. To limit the charging effect, an electron flood gun was used. The data were recorded in positive mode and ions combined with a Cs atom were followed for the depth profile.

X-ray photoelectron spectroscopy (XPS) was performed in a Thermo ESCALAB 250 Xi XPS system in order to study the chemical nature of the film bulk and interface. XPS was performed using an Al Kα source (1486.7 eV) with a 20 eV pass energy, while the XPS binding energy scale was calibrated by the adventitious C 1s peak at 285.0 eV. Curve fitting has been performed using CasaXPS ©; for 1s core peaks (O 1s, C 1s), a single peak has been used for each chemical environment while doublets have been used for 2p core peaks (Si 2p, Al 2p), accounting for spin-orbit coupling.

2.1. Island growth model presentation and validation

The computational model for island growth is inspired from the works of Nilsen et al. [20] and is based on geometric principles. The islands are assumed to be hemispherical due to the amorphous nature of the films [20], and grow on discrete nucleation sites. The nucleation sites are uniformly distributed, forming a square surface lattice. Due to the uniform distribution, the analysis is simplified to only one of the squares of the lattice, by imposing periodic boundary conditions.

The size of the squares from which the surface lattice is composed can be deduced from the nucleation density, N_d, which is the surface concentration of nucleation sites. If A is the area of the squares and b is their side length, then:

$$A = b^2 = \frac{1}{N_d} \quad (1)$$

$$b = \sqrt{\frac{1}{N_d}} \quad (2)$$

The thickness is computed as a mean thickness of the island over the whole square area A:

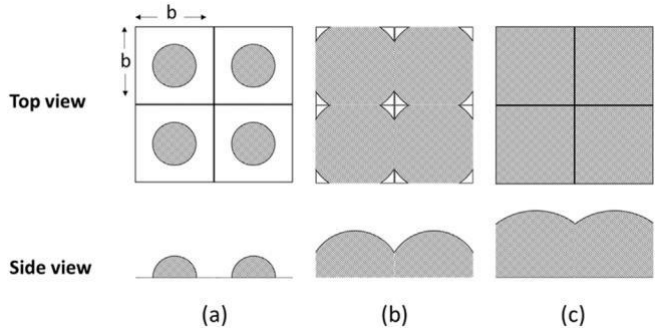

Fig. 1. Top and side view of the different regimes: a) free island growth b) island coalescence c) continuous film growth.

$$Thickness = \frac{Volume}{Area} = \frac{Volume}{A} \quad (3)$$

The island growth is divided into three regimes, illustrated in Fig. 1. The first regime is the free island growth regime, where the islands grow in hemispheres within the square lattice. The starting point for the second regime, island coalescence, is the moment when the island coalescence starts. The third regime, continuous film growth, starts when the whole surface is covered by the deposited film, hence when the film is continuous on the whole surface lattice. As the islands continue to grow and coalesce, this regime leads the ALD process to its steady state, where linear growth is obtained as a function of the ALD cycles.

The three regimes are taken into account in the geometric model. The critical island radius value for the transition from the first regime to the second is:

$$r_{c1\to2} = \frac{b}{2}, \quad (4)$$

While the critical value for the transition for the second regime to the third is:

$$r_{c2\to3} = \frac{\sqrt{2}\cdot b}{2} \quad (5)$$

Hence, the volume of the islands, is computed as follows:

If r_n is the island radius at the nth cycle:

For

$$r_n \le r_{c1\to2}$$

the island volume is equal to the volume of the hemisphere:

$$Volume = \frac{2\pi r_n^3}{3} \quad (6)$$

For

$$r_{c1\to2} \le r_n \le r_{c2\to3}$$

the island volume is equal to the volume of the hemisphere, minus four times the equivalent volume of half of a top spherical cap.

$$Volume = \frac{2\pi r_n^3}{3} - 4\cdot\frac{\int_{\frac{b}{2}}^{r_n}\pi(r^2 - z^2)dz}{2} \quad (7)$$

For

$$r_n \ge r_{c2\to3}$$

the film is continuous, and the island occupies the whole square. The volume of the island is:

$$Volume = \int_{-\frac{b}{2}}^{\frac{b}{2}}\int_{-\frac{b}{2}}^{\frac{b}{2}}\int_0^{\sqrt{r_n^2 - x^2 - y^2}} dz\,dx\,dy \quad (8)$$

Using the above model, the Growth per Cycle (GPC) evolution can be computed as a function of the number of ALD cycles, as follows:

$$GPC_n = Thickness_n - Thickness_{n-1} \quad (9)$$

The island radius at the nth cycle is given by:

$$r_n = r_{n-1} + \Delta r, \quad (10)$$

where r is the radius increase during each ALD cycle. Its value is equal to the GPC at the steady ALD regime, where the thickness is a linear function of the ALD cycles. This value is easily accessible by experi-mental measurements, once the steady ALD regime is reached. The initial island radius prior to ALD deposition, r_0, is a model parameter. Although it is usually taken as zero, it is nonetheless included for the generality of the model. Surface functionalization can lead to the pre-sence of nucleation sites with a radius of some number of Å.

The computational model has two fitting parameters, which are the nucleation density, N_d and the initial radius of the islands, r_0. The value of r_0 represents the apparent radius of a surface nucleation site. As nucleation sites are usually surface defect sites, r_0 varies from zero to some number of Å. Once this value is set, by tuning the values of N_d, an estimation of the surface concentration of nucleation sites can be de-rived, by fitting the model results to experimental data.

To demonstrate the validity of the model, we have compared its results with literature experimental data. It is worth noting that the model is independent of the deposited material, as long as it is amor-phous and the island growth indeed occurs. This is why we present a comparison between model predictions and literature data, for the ALD of Al_2O_3 on SieH [19], PtO_2 on Si with native SiO_2 [36], and W on SiO_2 [34] in Fig. 2. For all cases in Fig. 2, the initial radius value, r_0, was set to zero. The r values are taken from the slope of the thickness once the linear ALD regime is obtained.

The good agreement between model predictions and literature data in Fig. 2 proves that the model can be used to analyze the deposition during the first cycles, and extract an estimation of the nucleation density. The growth mode can be predicted and characterized, without using any chemical reactions, but only geometrical principles, using two fitting parameters. Hence, the initial growth evolution can be ex-plained by geometrical aspects of the film growth, without assuming an increasing surface reactivity with the number of ALD cycles. The growth regimes during the first steps of deposition can be separated and studied, as well as the transition between them. The nucleation density fitted for the data in Fig. 2 varies between 0.06 and 0.09 groups/nm^2. Nucleation densities derived from the fitting of such models to ex-perimental measurements have previously been assigned to surface defect sites [16,20].

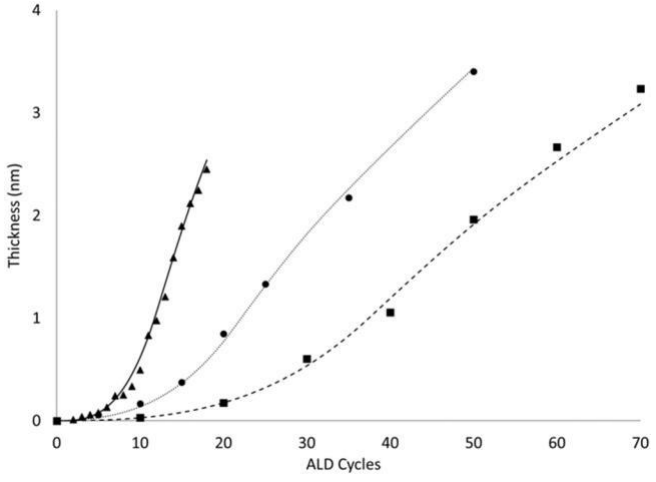

Fig. 2. Model predictions comparison with literature data, using $r_0 = 0$. Data from literature: Triangles: W on SiO_2, Elam et al. [34]. Circles: Al_2O_3 on Si, Besling et al. [19]. Squares: PtO_2 on SiO_2, Knoops et al. [36]. Model predictions: Continuous line: $N_d = 0.06$, r = 0.17 nm. Dotted line: $N_d = 0.09$, r = 0.07 nm. Dashed line: $N_d = 0.07$, r = 0.047 nm.

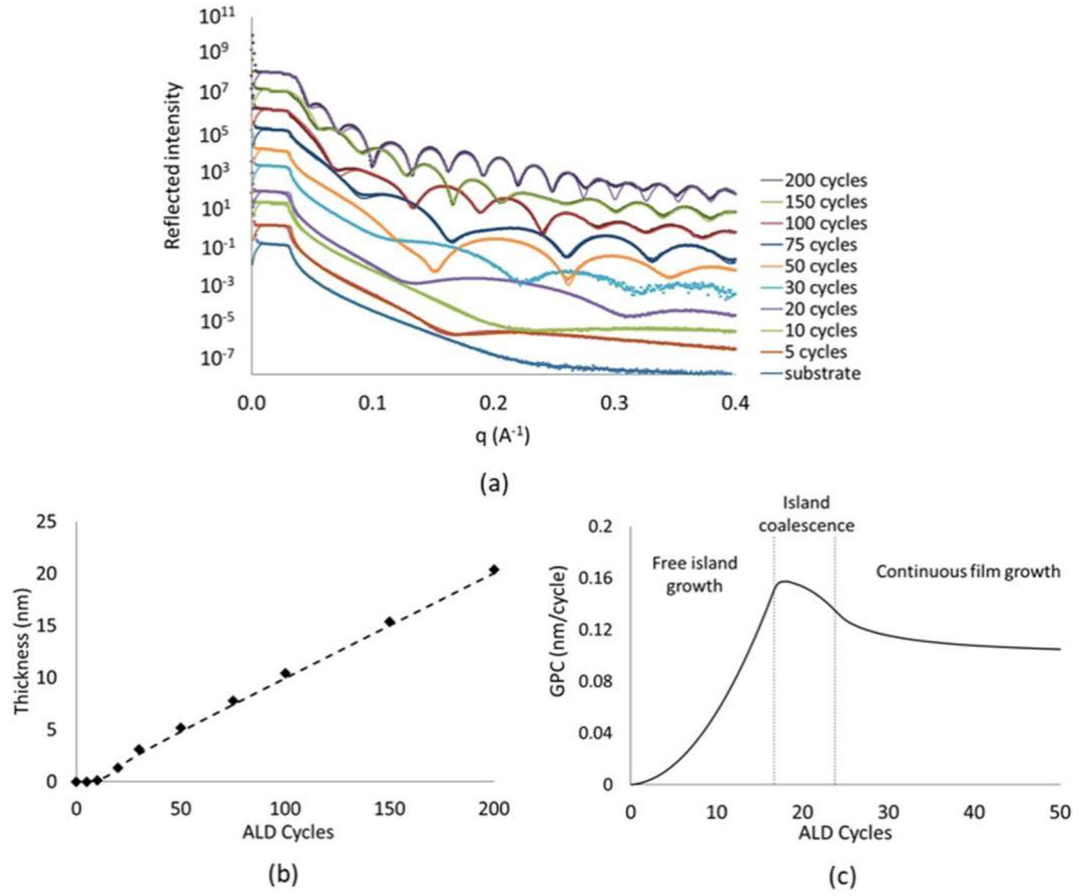

Fig. 3. a) XRR measurements and fit for 0 to 200 ALD cycles. b) Layer thicknesses derived from XRR fitting (rhombus) and comparison with island growth model predictions (dashed line) for the ALD of Al_2O_3 on a H-terminated Si substrate. c) Evolution of the GPC as a function of the number of cycles: model predictions, using r = 0.1 nm. Model fitting parameters: N_d = 0.08 groups per nm^2, r_0 = 0 nm.

3. Results and discussion

3.1. Evolution of Al_2O_3 growth

The ALD films using various numbers of cycles were characterized by XRR in order to determine their thickness. The XRR data were fitted using a matrix model (Parratt formalism [37]) by considering a fixed density of Al_2O_3 in the deposited layer in order to recover its thickness. XRR data and calculated curves are shown in Fig. 3a. The derived de-posited thickness is plotted in Fig. 3b as a function of the number of ALD cycles, along with the predictions of the island growth model. The predicted evolution of the GPC and the growth regimes are shown in Fig. 3c.

Results of Fig. 3b show that an induction period occurs during the initial stages of Al_2O_3 ALD on H-terminated Si. This behavior has been previously reported by Puurunen et al. [16,17] for the ALD of alumina on SiH. This is due to the low reactivity of the SiH species towards ALD reactants [30,35]. This low reactivity prevents TMA and H_2O from depositing on the surface.

Nucleation is reported to start on surface defect sites [16,17,30], such as surface OH groups or oxygen bridges that have not been totally removed during the substrate cleaning process. These defect surface species are reactive towards the ALD reactants, contrary to the SiH species. Then, subsequent exposure leads to preferential deposition of the reactants on the already deposited material and its adjacent surface sites [16,30], thus leading to the formation of islands, as assumed by the island growth model. The good agreement between the island growth model and the XRR measurements shows that indeed the sur-face inhibited growth and preferential deposition lead to an island growth regime during the first deposition steps.

The fitting of the model yields an estimation of the surface con-centration of the initial nucleation sites, i.e. the surface defect sites. The GPC at the steady ALD regime is 0.1 nm/cycle, which is consistent with our ellipsometry measurements and the mechanistic surface kinetics model we presented in our previous work, for the same ALD reactor [13]. Thus, by setting r = 0.1 nm, the resulting N_d value needed to fit the model to the XRR measurements is Nd = 0.08 groups/nm^2. If this value is assigned to OH groups, it is 1.27% of the surface concentration of OH groups on silica at 300 °C, as reported by Haukka and Root [33]. This means that the HF cleaning efficiently removes the native oxide layer.

As the number of cycles increases, island growth and coalescence occurs. The different regimes are dictated by the state of the growing islands and are shown by the characteristic evolution of the GPC in Fig. 3c. Islands growing freely on the surface increase the available surface for deposition and hence the GPC is enhanced. This occurs until $r = r_{c\,1\to2} = \frac{b}{2}$, as described in the previous section. In the present case, this happens after 18 ALD cycles. From the moment the islands start to coalesce, the surface available for deposition starts to decrease, until the formation of a continuous film. This happens when $r = r_{c\,2\to3} = \frac{\sqrt{2}\cdot b}{2}$, which in the present case is after 25 ALD cycles. This prediction is in agreement with the experimental observations of Puurunen et al. [16]. From then onwards, the coalescence continues, decreasing the surface available for deposition, and thus the GPC, until layer by layer growth is reached, where the GPC becomes constant. The above analysis shows that at least 25 ALD cycles must be performed, in order to obtain a continuous Al_2O_3 film. This approach also shows that the evolution of the film growth can be explained by the geometric

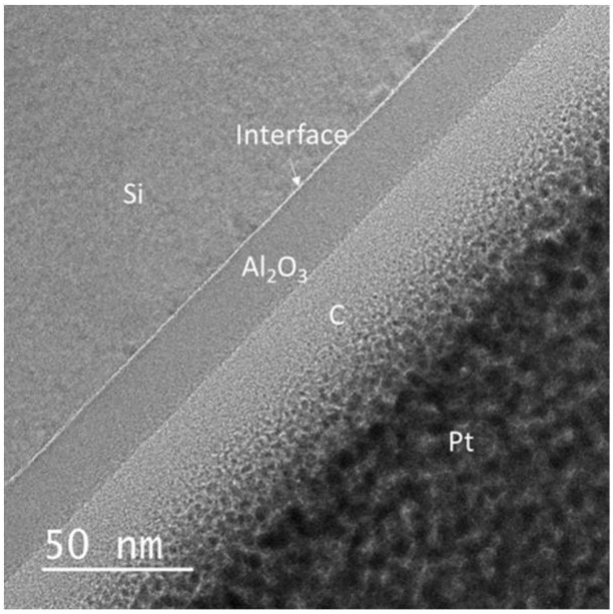

Fig. 4. TEM image of an ALD grown Al_2O_3 layer using 200 ALD cycles.

aspects of growth, without assuming an increasing surface reactivity with the number of ALD cycles.

3.2. Morphological characterizations of Al_2O_3 films

The obtained Al_2O_3 films after different numbers of ALD cycles were characterized by TEM and BF-STEM. The bulk of the Al_2O_3 is distinguished from the Si substrate and the C capping layer. The films are all amorphous, confirmed by fast Fourier Transform (FFT) analysis of the TEM images, in contrast to the crystalline Si substrate. The TEM analysis of the film grown after 200 ALD cycles is shown in Fig. 4.

It is seen that the Al_2O_3 film is uniform and conformal. It is distinguished by a darker contrast than both the Si substrate and the C capping layer. The ALD layer has a thickness of ~20.3 nm, yielding a mean GPC of ~0.1 nm/cycle. The GPC computed from our surface kinetic model [13], as well as the GPC derived from the island growth model and the XRR measurements are consistent with this measurement. This GPC of ~0.1 nm/cycle was also measured for the sample deposited using 550 ALD cycles.

An interfacial layer between the ALD grown film and the Si substrate is also observed in Fig. 4 as a bright-contrast layer. Literature reports conclude that this layer is either observable [26–28] or not observable [22] for the TMA + H_2O process. This interface is reported to mainly consist of Si oxides [4,24,25], formed by interdiffusion of Si and O species. To further investigate the interfacial layer morphology and film evolution, TEM and BF-STEM images of the Al_2O_3 films formed after 5, 20 and 200 ALD cycles are shown in Fig. 5. The films deposited using 5 and 20 ALD cycles were characterized by STEM in bright-field, for a more clear distinction of the interface.

For the sample deposited using 5 ALD cycles (Fig. 5a), the BF-STEM micrograph shows no clear distinction between an Al_2O_3 layer and the interface. According to the island growth model and the results of Puurunen et al. [16], the deposition is still in the nucleation period, where island growth takes place. A layer with a varying darker contrast could be argued to be present between the C layer and the brighter contrast interfacial oxide layer. It could be attributed to islands closely behind each other in the cross-sectional sample, giving the appearance of a continuous layer [16]. The layer's varying contrast consolidates this explanation. For this sample, a combined layer of ~1.6 nm is measured between the crystalline structure of the Si substrate and the brighter contrast of the C layer.

For films deposited using 20 and 200 cycles (Fig. 5b and c, respec-tively) the interfacial layer is clearly visible and can be distinguished from both the Si substrate and the Al_2O_3 layer. The measured Al_2O_3 and interface layer thicknesses by the TEM and BF-STEM analysis are summarized in Table 1 for all samples, as for a 550 cycles sample (not shown in Fig. 5).

An interface of ~1.8 nm was measured for the 20 cycles sample (Fig. 5b), while the 200 cycles sample showed an interface of ~2 nm (Fig. 5c). The interfacial layer thickness is close for both samples, which shows that between 20 and 200 cycles, little or no Si oxidation took place. So, after a certain thickness, the Al_2O_3 layer serves as a diffusion barrier for Si and O species. This has been previously reported for the Al_2O_3 deposition on Cr surfaces, where a thin thermal ALD Al_2O_3 layer was found to serve as an efficient diffusion barrier to prevent Cr oxi-dation during subsequent plasma enhanced ALD [29].

The 20 cycles sample (Fig. 5b) also exhibited a slightly higher roughness on its interface with the C capping layer. This is attributed to the end of the island growth mode. According to the island growth model, the island coalescence has started at that point and a continuous layer is obtained only after 25 cycles. The varying contrast along the layer in Fig. 5b, could be assigned to this phenomenon. In their work, Puurunen et al. [16] revealed the Al_2O_3 islands on Si, by in situ de-positing an amorphous Si layer on top of their samples. When the Al_2O_3 layer was not continuous, the deposited Si aligned epitaxially on the Si substrate, thus making the Al_2O_3 islands visible [16]. They estimated that the film becomes continuous between 20 and 30 cycles, in agree-ment with the predictions of the island growth model presented here.

3.3. Chemical characterization of the Al_2O_3 films

The deposited films were characterized by XPS, in order to study the chemical nature of the deposited films and their interfaces with Si. The Al 2p, O 1s and Si 2p spectra are presented in Fig. 6, for ALD films deposited using 10 and 50 ALD cycles. The intensity scales have been adjusted to highlight the different features of the spectra.

Fig. 6 shows that Al is detected on the surface even for the 10 ALD cycles sample. Although the intensity is lower than for the 50 cycles sample, the peak position is the same. The main peak is located at 74.8 eV and can be simulated by a doublet peak (Al $2p_{3/2}$: 74.8 eV, Al $2p_{1/2}$: 75.24 eV), showing the presence of O-Al-O bonds. The Al 2p peak for both samples could also be fitted by a single symmetrical peak at 74.8 eV. From the TEM analysis performed on the 10 cycles sample (not shown), the deposited layer could not be distinguished, probably due to the fact that the film growth is still in the island regime (as shown by the island growth model) and no continuous ALD layer has been de-posited on the surface. However, Fig. 6 shows a clear Al 2p peak, meaning that Al has already been deposited on the surface.

The O 1s spectra were fitted using a main peak at 531.8 eV, assigned to AleO bonds. A small contribution from a second peak at 533.3 eV was also used for the fitting. Renault et al. [4] attributed such a peak situated at E = 1.3–1.4 eV higher in energy than the main O 1s peak to Al-OH species. The presence of these species is consistent with the chemistry of TMA and H_2O [3,4,13]. TMA deposits on the surface in the form of $Al(CH_3)_x$ species. During the subsequent reactant exposure, H_2O reacts with the surface species, leading to the formation of Al-OH species, and CH_4 as a byproduct [3,4,13]. Non complete coverage of the AleOH species during the next TMA exposure can lead to the in-corporation of those AleOH species in the film bulk. For a detailed understanding of the TMA + H_2O chemistry, the reader is referred to our previous work [13].

The Si 2p spectra presented in Fig. 6 show the chemical nature of the interface. For both samples, a clear doublet peak is situated at 98.9 eV (Si $2p_{3/2}$: 98.84 eV, Si $2p_{1/2}$: 99.47 eV), which is attributed to elemental Si^0. This shows that the depth of the analysis reaches the Si substrate, for the 10 and 50 cycles samples. A second peak is situated at 102.3 eV (Si $2p_{3/2}$: 102.04 eV, Si $2p_{1/2}$: 102.67 eV), for both samples, to

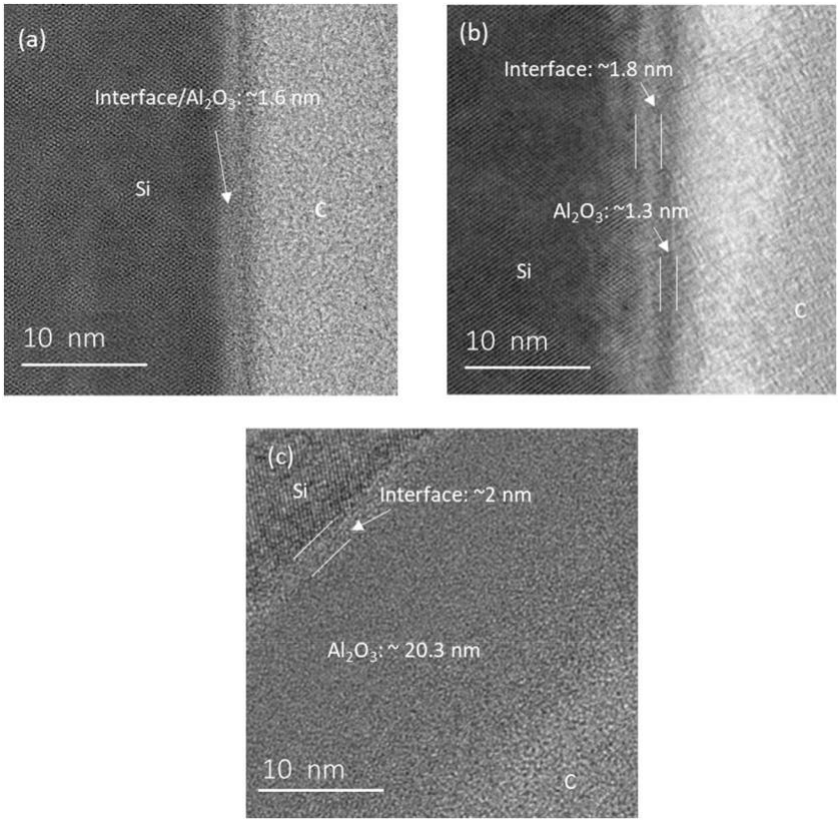

Fig. 5. TEM and BF-STEM images of ALD grown Al_2O_3 layers using: a) 5 (BF-STEM), b) 20 (BF-STEM), c) 200 (TEM) ALD cycles.

Table 1

Experimental thickness of the Al_2O_3 film and of the interfacial layer measured by TEM and BF-STEM, for all samples.

No. of ALD cycles	Al_2O_3 thickness (nm)	Interface thickness (nm)
5	1.6 (impossible to distinguish between film and interface)	
20	~1.3	~1.8
200	~20.3	~2
550	~55.4	~2

a E = 3.4 eV from the Si^0 peak. This E value assigns this peak to Si of higher oxidation states, such as Si^{3+} and Si^{4+}. In Fig. 6, this peak has been fitted by a doublet peak. However, different deconvolution schemes have been presented in the literature. By using the data treatment of Renault et al. [4], a peak at E = 3.01 eV is found in our results, between the Si^{4+} and Si^{2+} peaks. This peak has a E that is too high to be assigned to Si^{3+}, and has previously been attributed to Al-silicate bonds by Renault et al. [4] This analysis concludes in the ex-istence of multiple oxidation states of Si at the interface, including Si^{3+}, as well as to the presence of Al-silicates [4].

In order to study the elemental composition along the film depth, probing of Al, Si, and O species was performed by EDX on TEM cross sections. Measurements were performed along a straight line perpen-dicular to the sample surface, starting from the Si substrate and the obtained elemental profiles, excluding carbon, are shown in Fig. 7 for samples after 5, 20 and 200 ALD cycles. In order to study the passi-vation efficiency of the Si substrate pre-treatment, the EDX measure-ments along the film depth are also shown for the Si substrate without Al_2O_3 deposition in Fig. 7. Although this analysis is qualitative, it provides valuable insight for the evolution of the film and of the in-terface.

A very small rise on the O counts is detected on the Si surface (in-terface between Si substrate and C capping layer), for the substrate sample without deposition (Fig. 7a). This shows that the HF cleaning of the substrate removes the majority of surface oxides, leaving the surface H-terminated. The SieH surface is passivated towards oxidation. Frank et al. [30] showed that the SieH surface does not react with deuterated water, D_2O, even after repeated D_2O exposures [30]. They report a weak O presence on H-terminated Si(100) substrates, attributed to defect sites (SieOH) remaining on the surface after the substrate cleaning due to the higher atomic roughness of the Si(100) surface [30]. Halls et al. [35] performed theoretical studies using DFT calculations on the H-terminated Si surface reactions with TMA and H_2O [35]. Their results confirm the low reactivity of the surface towards both reactants.

We therefore assign the small amount of detected O on the surface to such surface defect sites, like O bridges or SieOH groups that have not been appropriately removed, or to SiO_x formed after the sample exposure to air. The ALD nucleation during the first ALD cycles is re-ported to take place on such defects [16,17,30]. Our island growth model, fitted to the XRR measurements, estimates the surface con-centration of those defects at 0.08 groups/nm^2. The ALD film starts forming on those defects. Then, subsequent deposition of Al on the surface catalyzes further Al_2O_3 deposition on nearby sites, as well as localized substrate oxidation, under and around the deposited Al_2O_3 [30,31].

This effect is seen on the Al, O, Si profiles on a 5 ALD cycle Al_2O_3 sample on Fig. 7b. In this case, between the Si substrate and the C layer, a clear peak on the O counts is observed, together with a small peak of Al. The presence of Al was also detected by XPS on a 10 cycle Al_2O_3 sample (Fig. 6). These results show that after 5 cycles, only a very small amount of Al has been deposited. This is consistent with the island growth model results and XRR measurements. After 5 cycles, the film deposition is still in its nucleation period and only small Al_2O_3 islands are deposited. However, even on the 5 cycle sample (Fig. 7b), the O peak is more significant than on the substrate sample (Fig. 7a). Starting from the Si substrate and moving to the C layer, we notice that the O

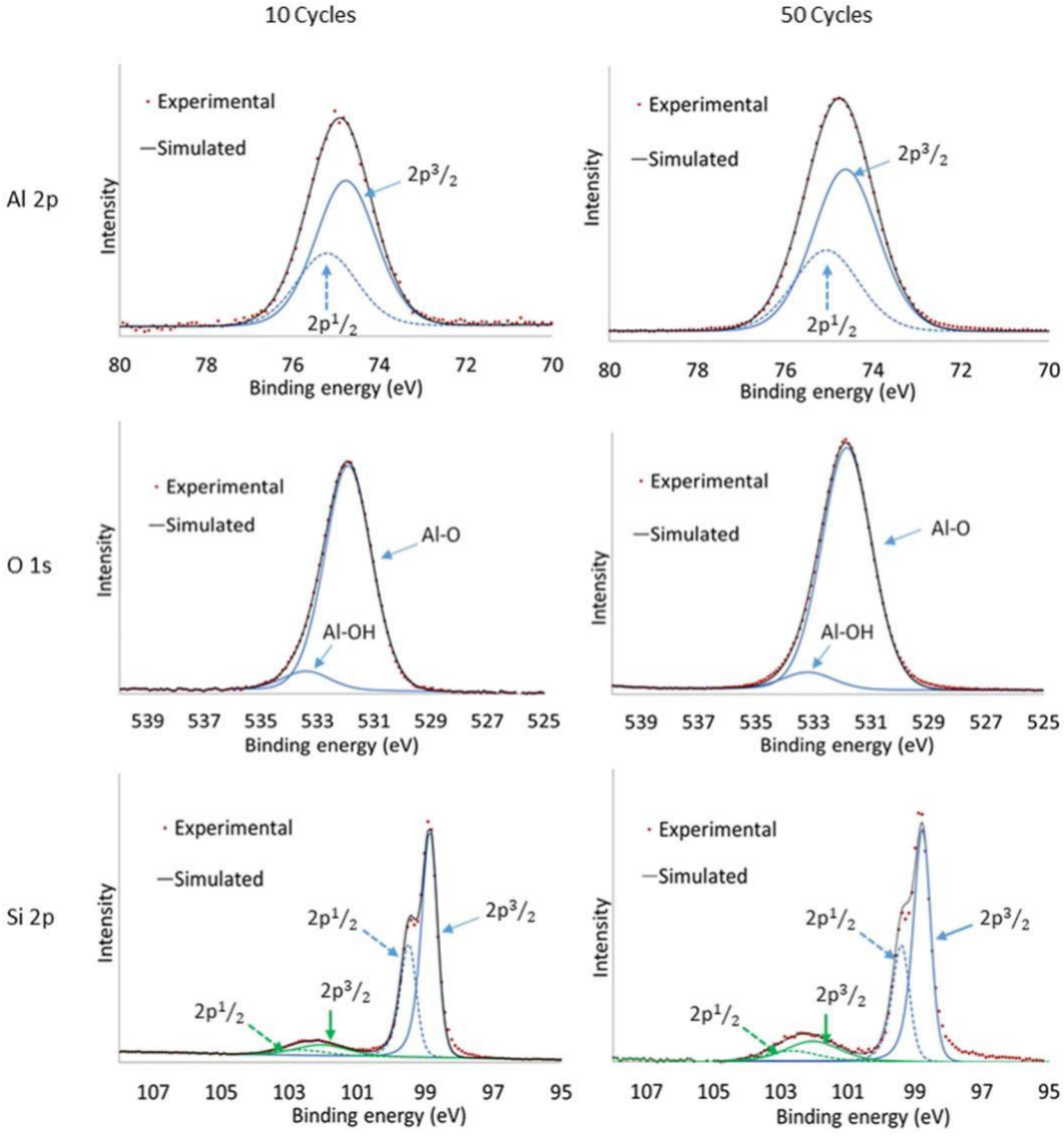

Fig. 6. Al 2p (top), O 1 s (middle) and Si 2p (bottom) XPS spectra for Al_2O_3 films deposited using 10 (left) and 50 (right) ALD cycles.

counts increase before the appearance of Al. This is attributed to the oxidation of the Si substrate, with an oxidation of the Si substrate under the Al_2O_3 deposition. However, it is not evident if this oxidation is in-herent to the ALD process or if it is due to subsequent oxidation after the sample exposure to air. In both cases, this result shows that the Al deposition enhances Si oxidation, even at low Al surface concentration [30,31]. Frank et al. [30] also showed that after the first TMA pulse, subsequent D_2O exposures lead to subsurface oxidation of Si [30]. By using the full width at half maximum (FWHM) of the element count peaks, we can estimate the total thickness of the oxidized layer at ~1.93 nm, of which ~1.63 nm consist of SiO_x with no traces of Al, while the thickness where Al was traced is ~0.3 nm. These values show a slightly higher thickness of the oxidized layer than in Table 1.

Fig. 7c shows an Al_2O_3 sample deposited with 20 ALD cycles. The clear Al and O peaks in the profile are due to the deposition of Al_2O_3. Our island growth analysis shows that after 20 cycles, the growth re-gime is near the end of the island growth regime; however non con-tinuity of the film was still predicted. By using the FWHM of the ele-ment count peaks, we deduce a region of ~1.5 nm, where only Si and O species are present, thus the formation of a SiO_x layer. A ~0.7 nm re-gion, where Si, O and Al species are all present, then is detected before the Al_2O_3 layer. This region can consist of Al-silicates or SiO_x and AlO_x.

The presence of Al-silicates has also been reported before [4], and is one possible conclusion from the XPS analysis of the present work (Fig. 6). The total thickness of the interface containing Si is 2.2 nm, slightly higher than the one measured by TEM (Table 1).

The proposed mechanism for the Si oxide formation is the diffusion of O species from the deposited Al_2O_3 film [29], leading to Si oxidation. However, the reaction of H_2O with surface Si groups during the island growth where the surface is not fully covered by the ALD film, catalyzed by the presence of Al [30,31], has also been suggested as a mechanism for the interfacial oxide growth [24,30]. Naumann et al. [24] reported that the OH groups formed during the initial island growth, lead to the formation of SiOH species. These species lead to further substrate oxi-dation after further increase of the ALD cycles. Xu et al. showed that by using a long exposure to TMA prior to ALD deposition, the interfacial Si oxide thickness is strongly restricted due to the covering of a larger fraction of the surface by Al species. The diffusion of O through the ALD layer is also a possible source of oxidation, which is however limited as the ALD film continues to grow due to the presence of Al_2O_3 as a dif-fusion barrier. Thus, oxidation by H_2O and surface OH groups of the non-covered Si surface is restricted. As shown by Halls and Ragha-vachari [35], although the overall reaction between the ALD reactants and SieH surface species is thermodynamically possible, the reactivity

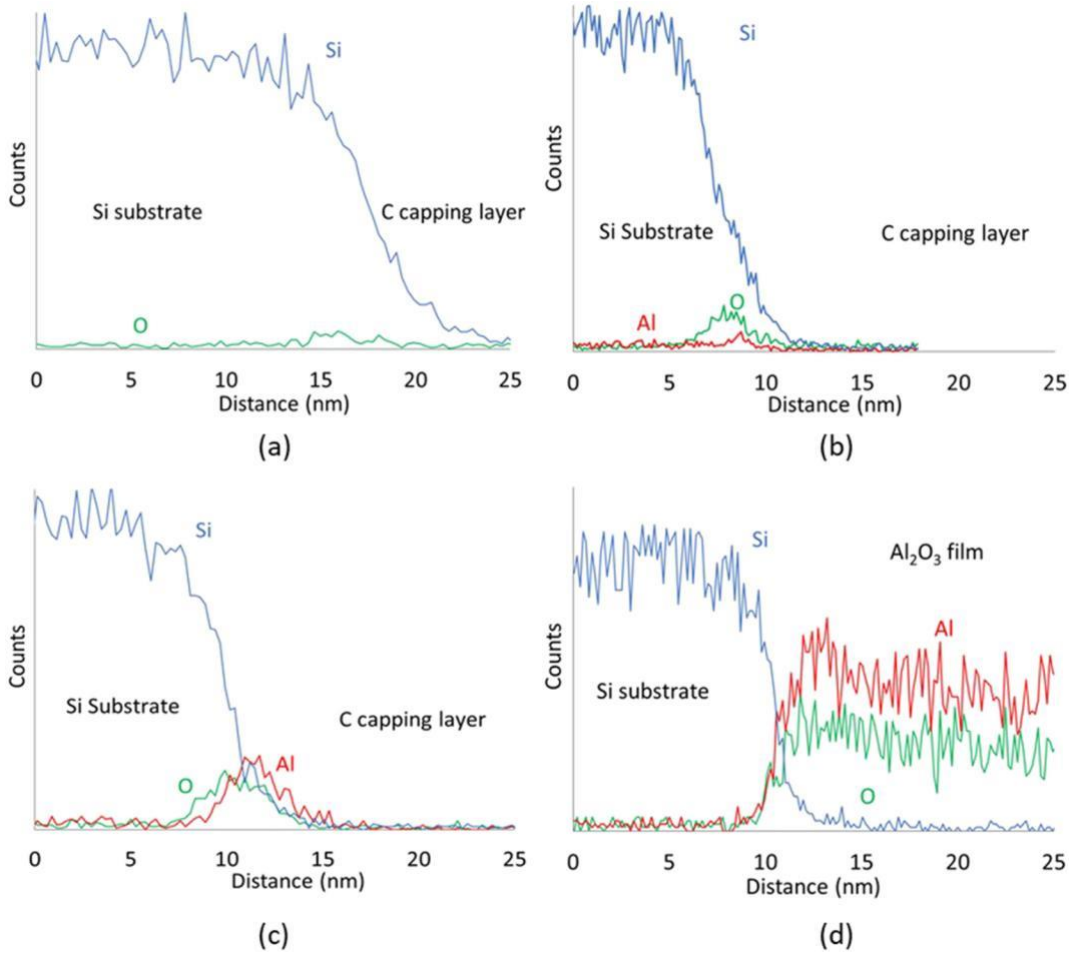

Fig. 7. EDX measurements along the film depth for a) Si substrate without ALD b) 5 ALD cycles Al_2O_3 c) 20 ALD cycles Al_2O_3 d) 200 ALD cycles Al_2O_3.

is very low due to the high energy barrier required. Xu et al. [27,28] use a very long (3600 s) TMA exposure of the SiH surface prior to de-position. Such a long exposure may be long enough for the reactants to react and deposit on the surface, covering a large fraction of the surface, thus restricting the induction period. However, for industrial applica-tions, performing such exposures is challenging and costly, as proces-sing time is highly increased and deposition takes place on all the re-actor walls. Furthermore, the duration of the reactor purging, needed to ensure that no TMA is left in the chamber before starting the ALD process, would be extremely long. In our case, the exposure times are in the order of ms, and more than 10^5 times smaller than in the case of Xu et al. [27,28] Hence, the reactions between the ALD reactants and the SiH surface do not occur. The ALD reactants deposit only on surface defect sites. During subsequent cycles, the ALD reactants deposit pre-ferentially on and around already deposited material, leading to island growth.

The EDX elemental profiles for the sample deposited using 200 ALD cycles shown in Fig. 7d, reveal the several nm thick Al_2O_3 film. Within the bulk of the Al_2O_3 film, a uniform Al and O concentration is mea-sured by quantitative analysis (not shown), with a Al/O ratio close to the Al_2O_3 stoichiometry.

In the 5 and 20 cycles samples, the O peak is present even before the appearance of Al in the interface. This is not the case for the 200 cycle sample, where Si, O and Al species are present all along the interface. For the 5 and 20 cycles samples, the Al_2O_3 film may not be continuous and a part of the Si surface is directly exposed to atmospheric O, and thus oxidized. Therefore, the 20 nm thick Al_2O_3 film deposited for the 200 cycles sample serves as an effective diffusion barrier against O diffusion through the layer and prevents further Si oxidation by ambient air. Using the FWHM of the count peaks, we deduce a 1.2 nm interface, containing Si, O and Al. This value is smaller than the one measured by TEM (Table 1).

ToF-SIMS allows detailed investigation of the chemical composition of the film along its depth. Fig. 8 shows the elemental profile of the 200 cycles sample from the surface to the substrate.

The SIMS analysis shows a uniform concentration profile for Al and O species in the core of the film, where no Si is detected. This confirms that during the stable ALD regime, the Al_2O_3 film is deposited with

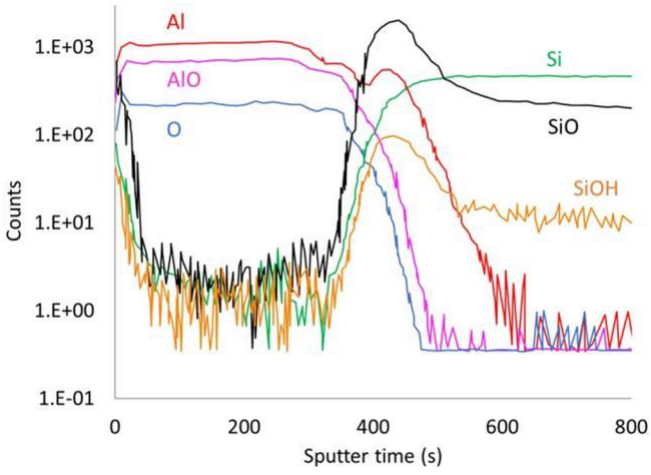

Fig. 8. SIMS depth profiles for the 200 ALD cycles sample.

constant composition during each cycle. The surface is regenerated after the end of each ALD cycle, and the deposition process is repeated.

When the sputtering reaches the interface, the AlO and O counts decrease, until the Si substrate is reached, where AlO and O are no longer detected. The Si signal has the opposite behavior: Si counts start to increase at the same sputtering time where the AlO and O counts decrease, until the Si substrate is reached where the Si counts remain constant. The behavior of Al counts is different since they start to de-crease when sputtering reaches the interface, as in the case of AlO and O. Then, the Al counts increase exhibiting a small peak in the interface, before decreasing to zero in the Si substrate region. This leads to the distinction of two regions in the interface: an Al depleted region at the top of the interface, closer to the core of the ALD film, and an Al en-riched region, in the interface. The different behavior of the Al and AlO depth profiles within the interface witnesses a possible different che-mical environment of Al within the interface showing that Al could be present in the interface in states different from Al_2O_3, such as Al-sili-cates. Gosset et al. [25] also performed SIMS characterizations on ALD deposited AlO_3 on H-terminated Si. They observed a similar behavior for the Al and OH species at the interface. After annealing in N_2 at 800 °C and 1000 °C, they observed Al and H diffusion from the interface towards the film bulk. Al diffusion from the interface towards the sur-face during thermal annealing has also been shown by Krug et al. [32].

The SiO and SiOH depth profiles also show a similar behavior: in the interface, SiO and SiOH counts increase, exhibiting a peak of their concentrations, before decreasing as the Si substrate is reached by the sputtering. These peaks appear at the same position as the Al peak, thus confirming that within the interface a different chemical environment of Al is present. These results show that Al, O, Si species are all present within the film interface, as was shown by EDX results in Fig. 7. The interface, formed by interdiffusion and reaction of species during the first ALD cycles, is hence a mixture of SiO_x, AlO_x and SiOH. The pre-sence of Al silicates is also possible, as discussed in the XPS analysis (Fig. 6).

Al-OH groups have been suggested to enhance O diffusion and Si oxidation [25], as bulk defect sites. The analysis of the O 1s spectra from XPS (Fig. 6) showed a small peak that has previously been as-signed [4] to AleOH bonds. The SIMS results of Fig. 8, reveal the presence of the SiOH groups in the interface. This presence could be the source of the substrate oxidation during the island growth regime [24]. The SiOH groups are formed during the island growth regime that takes place during the first cycles of deposition. The mechanism for their formation could be the reaction of AleOH species created from the ALD surface chemistry [3,6,7,10,13] with Si surface species, which are non-fully covered by Al species during the island growth.

4. Conclusions

In this work, the ALD of Al_2O_3 films from TMA and H_2O was studied on H-terminated Si (100) substrates, in a commercial reactor with the purpose to thoroughly investigate the initial film deposition evolution and interface formation. A series of samples using a different number of ALD cycles were deposited at 300 °C. The films and their interface with the substrate were characterized by XRR, TEM, BF-STEM, XPS, EDX and ToF-SIMS. A geometrical island growth model based on the work of Nilsen et al. [20] was used to reproduce the nucleation and growth steps during the first cycles. The model succeeded in representing the Al_2O_3 thickness evolution during the first ALD cycles, without involving the modelling of surface reactions. This approach showed that the evolution of the film growth can be explained by the geometric aspects of growth, without assuming an increasing surface reactivity during the first ALD cycles. It allowed the estimation of the surface concentration of defect sites, such as Si-OH and O bridges on the initial Si surface as close to 0.08 groups/nm^2 and revealed that 25 ALD cycles are needed to achieve film continuity.

Concomitant results by TEM, BF-STEM, XPS, SIMS and EDX also showed that an interfacial layer was formed between the Al_2O_3 film and the Si substrate. This layer consists of oxidized Si in various oxidation states, while Al is also present, suggesting the presence of AlO_x and Al-silicates. In agreement with the reported results, the interfacial layer formation starts with the Al_2O_3 film during the first cycles. The me-chanisms involve Si oxidation during the first cycles, when island growth takes place, and the surface is not fully covered by the Al_2O_3 film. Although this oxidation was highly restricted for the H-terminated Si surface, the presence of Al on the surface catalyzes Si oxidation, and thus the interfacial layer formation. This oxidation could occur through the formation of SiOH groups during the island growth. These SiOH groups could be formed from the reaction of OH species on the de-posited islands with non-covered Si on the surface. SIMS results vali-dated the presence of SiOH groups in the interface, thus further con-solidating this assumption. Once the whole surface is covered by the ALD film, the interfacial oxide layer may continue to grow due to in-terdiffusion of O species through the layer. This interdiffusion has been assigned to bulk defect species, present in the form of AlOH, facilitating the oxygen diffusion.

These results can serve as guidance towards the research of ade-quate surface pre-treatment techniques for silicon substrates, aiming to enhance their surface reactivity towards the ALD reactants, and restrict silicon oxidation. The development of such pre-treatments will pave the way to successfully produce continuous ALD layers with thicknesses down to 3 nm and abrupt interfaces with Si, for future nanoelectronics.

Acknowledgements

This work was partly funded by a Toulouse Tech Inter Lab 2016 grant and a Toulouse INP support. GPG acknowledges the financial support by the NTUA Research Committee. We are indebted to C. Josse, A. Pugliara and T. Hungria (UMS Castaing) for their help with sample characterization.

References

[1] R.W. Johnson, A. Hultqvist, S.F. Bent, A brief review of atomic layer deposition: from fundamentals to applications, Mater. Today 17 (2014) 236–246, https://doi.org/10.1016/j.mattod.2014.04.026.

[2] S.M. George, Atomic layer deposition: an overview, Chem. Rev. 110 (2010) 111–131, https://doi.org/10.1021/cr900056b.

[3] R.L. Puurunen, Surface chemistry of atomic layer deposition: a case study for the Trimethylaluminum/water process, J. Appl. Phys. 97 (2005) 121301, , https://doi.org/10.1063/1.1940727.

[4] O. Renault, L.G. Gosset, D. Rouchon, A. Ermolieff, Angle-resolved X-ray photo-electron spectroscopy of ultrathin Al_2O_3 films grown by atomic layer deposition, J. Vac. Sci. Technol. A 20 (2002) 1867–1876, https://doi.org/10.1116/1.1507330.

[5] J.D. Ferguson, A.W. Weimer, S.M. George, Atomic layer deposition of Al_2O_3 and SiO_2 on BN particles using sequential surface reactions, Appl. Surf. Sci. 162 (2000) 280–292, https://doi.org/10.1016/S0169-4332(00)00205-1.

[6] V. Vandalon, W.M.M. Kessels, What is limiting low-temperature atomic layer de-position of Al_2O_3? A vibrational sum-frequency generation study, Appl. Phys. Lett. 108 (2016) 011607, , https://doi.org/10.1063/1.4939654.

[7] V. Vandalon, W.M.M. Kessels, Revisiting the growth mechanism of atomic layer deposition of Al_2O_3: a vibrational sum-frequency generation study, J. Vac. Sci. Technol. A 35 (2017) 4993597, , https://doi.org/10.1116/1.4993597.

[8] D.-H. Kim, S.-B. Baek, Y.-C. Kim, Energy barriers for trimethylaluminum reaction with varying surface hydroxyl density, Appl. Surf. Sci. 258 (2011) 225–229, https://doi.org/10.1016/j.apsusc.2011.08.035.

[9] Y. Widjaja, C.B. Musgrave, Quantum chemical study of the mechanism of aluminum oxide atomic layer deposition, Appl. Phys. Lett. 80 (2002) 3304–3306, https://doi.org/10.1063/1.1473237.

[10] S. Seo, T. Nam, H.B.R. Lee, H. Kim, B. Shong, Molecular oxidation of surface –CH_3 during atomic layer deposition of Al_2O_3 with H_2O, H_2O_2, and O_3: a theoretical study, Appl. Surf. Sci. 457 (2018) 376–380, https://doi.org/10.1016/j.apsusc.2018. 06.160.

[11] R.L. Puurunen, Correlation between the growth-per-cycle and the surface hydroxyl group concentration in the atomic layer deposition of aluminum oxide from tri-methylaluminum and water, Appl. Surf. Sci. 245 (2005) 6–10, https://doi.org/10.1016/j.apsusc.2004.10.003.

[12] C.D. Travis, R.A. Adomaitis, Modeling ALD surface reaction and process dynamics using absolute reaction rate theory, Chem. Vap. Depos. 19 (2013) 4–14, https://doi.org/10.1002/cvde.201206985.

[13] G.P. Gakis, H. Vergnes, E. Scheid, C. Vahlas, A.G. Boudouvis, B. Caussat, Detailed investigation of the surface mechanisms and their interplay with transport

phenomena in alumina atomic layer deposition from TMA and water, Chem. Eng. Sci. 195 (2019) 399–412, https://doi.org/10.1016/j.ces.2018.09.037.
[14] G.P. Gakis, H. Vergnes, E. Scheid, C. Vahlas, B. Caussat, A.G. Boudouvis, Computational fluid dynamics simulation of the ALD of alumina from TMA and H_2O in a commercial reactor, Chem. Eng. Res. Des. 132 (2018) 795–811, https://doi.org/10.1016/j.cherd.2018.02.031.
[15] P. Peltonen, V. Vuorinen, G. Marin, A.J. Karttunen, M. Karppinen, Numerical study on the fluid dynamical aspects of atomic layer deposition process, J. Vac. Sci. Technol. A 36 (2018) 021516, , https://doi.org/10.1116/1.5018475.
[16] R.L. Puurunen, W. Vandervorst, W.F.A. Besling, O. Richard, H. Bender, T. Conard, C. Zhao, A. Delabie, M. Caymax, S. De Gendt, M. Heyns, M.M. Viitanen, M. De Ridder, H.H. Brongersma, Y. Tamminga, T. Dao, T. De Win, M. Verheijen, M. Kaiser, M. Tuominen, Island growth in the atomic layer deposition of zirconium oxide and aluminum oxide on hydrogen-terminated silicon: growth mode modeling and transmission electron microscopy, J. Appl. Phys. 96 (2004) 4878–4889, https://doi.org/10.1063/1.1787624.
[17] R.L. Puurunen, W. Vandervorst, Island growth as a growth mode in atomic layer deposition: a phenomenological model, J. Appl. Phys. 96 (2004) 7686–7695, https://doi.org/10.1063/1.1810193.
[18] M. Cassir, F. Goubin, C. Bernay, P. Vernoux, D. Lincot, Synthesis of ZrO_2 thin films by atomic layer deposition: growth kinetics, structural and electrical properties, Appl. Surf. Sci. 193 (2002) 120–128, https://doi.org/10.1016/S0169-4332(02) 00247-7.
[19] W.F.A. Besling, E. Young, T. Conard, C. Zhao, R. Carter, W. Vandervorst, M. Caymax, S. De Gendt, M. Heyns, J. Maes, M. Tuominen, S. Haukka, Characterisation of ALCVD Al_2O_3-ZrO_2 nanolaminates, link between electrical and structural properties, J. Non-Cryst. Solids 303 (2002) 123–133, https://doi.org/10. 1016/S0022-3093(02)00969-9.
[20] O. Nilsen, C.E. Mohn, A. Kjekshus, H. Fjellvåg, Analytical model for island growth in atomic layer deposition using geometrical principles, J. Appl. Phys. 102 (2007) 024906, , https://doi.org/10.1063/1.2756514.
[21] M.D. Groner, J.W. Elam, F.H. Fabreguette, S.M. George, Electrical characterization of thin Al_2O_3 films grown by atomic layer deposition on silicon and various metal substrates, Thin Solid Films 413 (2002) 186–197, https://doi.org/10.1016/S0040-6090(02)00438-8.
[22] S.C. Ha, E. Choi, S.H. Kim, J.S. Roh, Influence of oxidant source on the property of atomic layer deposited Al_2O_3 on hydrogen-terminated Si substrate, Thin Solid Films 476 (2005) 252–257, https://doi.org/10.1016/j.tsf.2004.09.035.
[23] J.C. Lee, S.J. Oh, Nondestructive depth profile of the chemical state of ultrathin Al_2O_3/Si interface, Appl. Phys. Lett. 84 (2004) 3561–3563, https://doi.org/10.1063/1.1734684.
[24] V. Naumann, M. Otto, R.B. Wehrspohn, C. Hagendorf, Chemical and structural study of electrically passivating Al_2O_3 /Si interfaces prepared by atomic layer de-position, J. Vac. Sci. Technol. A 30 (2012) 04D106, , https://doi.org/10.1116/1. 4704601.
[25] L.G. Gosset, J.F. Damlencourt, O. Renault, D. Rouchon, P. Holliger, A. Ermolieff, I. Trimaille, J.J. Ganem, F. Martin, M.N. Séméria, Interface and material characterization of thin Al_2O_3 layers deposited by ALD using TMA/H_2O, J. Non-Cryst. Solids 303 (2002) 17–23, https://doi.org/10.1016/S0022-3093(02)00958-4.
[26] Y. Chang, F. Ducroquet, E. Gautier, O. Renault, J. Legrand, J.F. Damlencourt, F. Martin, Surface preparation and post thermal treatment effects on interface properties of thin Al_2O_3 films deposited by ALD, Microelectron. Eng. 72 (2004) 326–331, https://doi.org/10.1016/j.mee.2004.01.012.
[27] M. Xu, C. Zhang, S.J. Ding, H.L. Lu, W. Chen, Q.Q. Sun, D.W. Zhang, L.K. Wang, Mechanism of interfacial layer suppression after performing surface $Al(CH_3)_3$ pre-treatment during atomic layer deposition of Al_2O_3, J. Appl. Phys. 100 (2006) 106101, , https://doi.org/10.1063/1.2388044.
[28] M. Xu, C.H. Xu, S.J. Ding, H.L. Lu, D.W. Zhang, L.K. Wang, Spectroscopic and electrical properties of atomic layer deposition Al_2O_3 gate dielectric on surface pretreated Si substrate, J. Appl. Phys. 99 (2006) 074109, , https://doi.org/10.1063/1.2187409.
[29] A. Foroughi-Abari, K.C. Cadien, In situ spectroscopic ellipsometry study of plasma-enhanced ALD of Al_2O_3 on chromium substrates, J. Electrochem. Soc. 159 (2012) D59–D64, https://doi.org/10.1149/2.035202jes.
[30] M.M. Frank, Y.J. Chabal, G.D. Wilk, Nucleation and interface formation mechan-isms in atomic layer deposition of gate oxides, Appl. Phys. Lett. 82 (2003) 4758–4760, https://doi.org/10.1063/1.1585129.
[31] S.W. Lim, F. Machuca, H. Liao, R.P. Chiarello, R.C. Helms, Effect of initial Al contamination on ultrathin gate oxides, J. Electrochem. Soc. 147 (2000) 1136–1140, https://doi.org/10.1149/1.1393325.
[32] C. Krug, E.B.O. Da Rosa, R.M.C. De Almeida, J. Morais, I.J.R. Baumvol, T.D.M. Salgado, F.C. Stedile, Atomic transport and chemical stability during annealing of ultrathin Al_2O_3 films on Si, Phys. Rev. Lett. 85 (2000) 4120–4123, https://doi.org/10.1103/PhysRevLett.85.4120.
[33] S. Haukka, A. Root, The reaction of hexamethyldisilazane and subsequent oxidation of trimethylsilyl groups on silica studied by solid-state NMR and FTIR, J. Phys. Chem. 98 (1994) 1695–1703, https://doi.org/10.1021/j100057a025.
[34] J.W. Elam, C.E. Nelson, R.K. Grubbs, S.M. George, Nucleation and growth during tungsten atomic layer deposition on SiO_2 surfaces, Thin Solid Films 386 (2001) 41–52, https://doi.org/10.1016/S0040-6090(01)00762-3.
[35] M.D. Halls, M.D., K. Raghavachari, Atomic layer deposition of Al_2O_3 on H-passi-vated Si. I. Initial surface reaction pathways with H/Si(100)-2×1, J. Chem. Phys. 118 (2003) 10221–10226. doi:https://doi.org/10.1063/1.1571513.
[36] H.C.M. Knoops, A.J.M. MacKus, M.E. Donders, M.C.M. Van De Sanden, P.H.L. Notten, W.M.M. Kessels, Remote plasma ALD of platinum and platinum oxide films, Electrochem. Solid-State Lett. 12 (2009) G34–G36, https://doi.org/10.1149/1.3125876.
[37] G. Vignaud, A. Gibaud, REFLEX: a program for the analysis of specular X-ray and neutron reflectivity data, J. Appl. Crystallogr. 52 (2019) 201–213, https://doi.org/10.1107/S1600576718018186.